

Dynamical approach to MPI 4 jet, W+dijet and Z+dijet production in Pythia 8

B.Blok and P.Gunnellini

Based on •

- [Dynamical approach to MPI four-jet production in Pythia](#)
[B. Blok \(Technion\)](#), [P. Gunnellini \(DESY\)](#). Published in **Eur.Phys.J. C75 (2015) 6, 282**
e-Print: [arXiv:1503.08246 \[hep-ph\]](#) |

[Dynamical approach to MPI in W+dijet and Z+dijet production within the PYTHIA event generator](#)

[B. Blok, P. Gunnellini](#). Oct 26, 2015.
e-Print: [arXiv:1510.07436 \[hep-ph\]](#) |



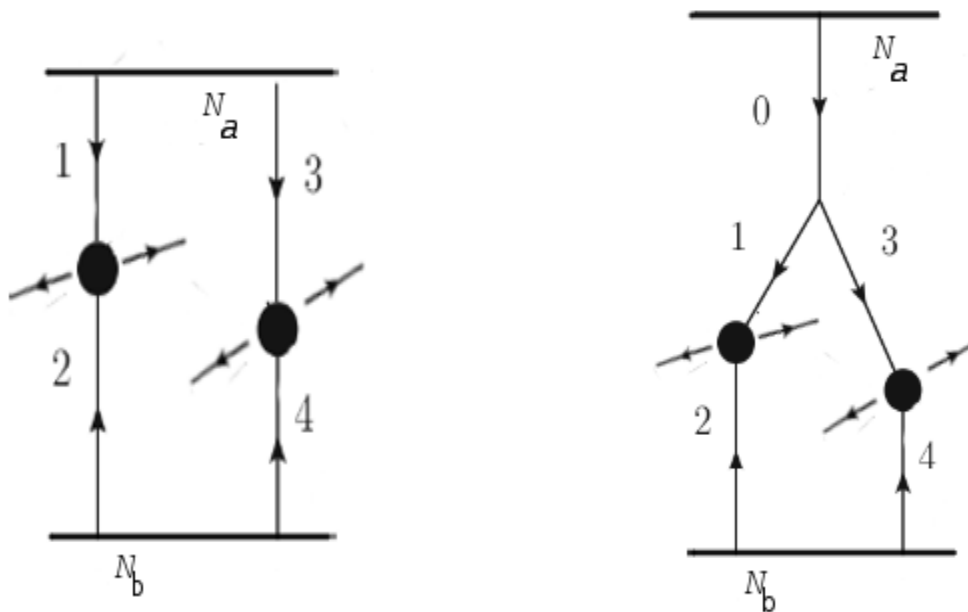


FIG. 1: Sketch of the two considered MPI mechanisms: $2 \otimes 2$ (left) and $1 \otimes 2$ (right) mechanism.

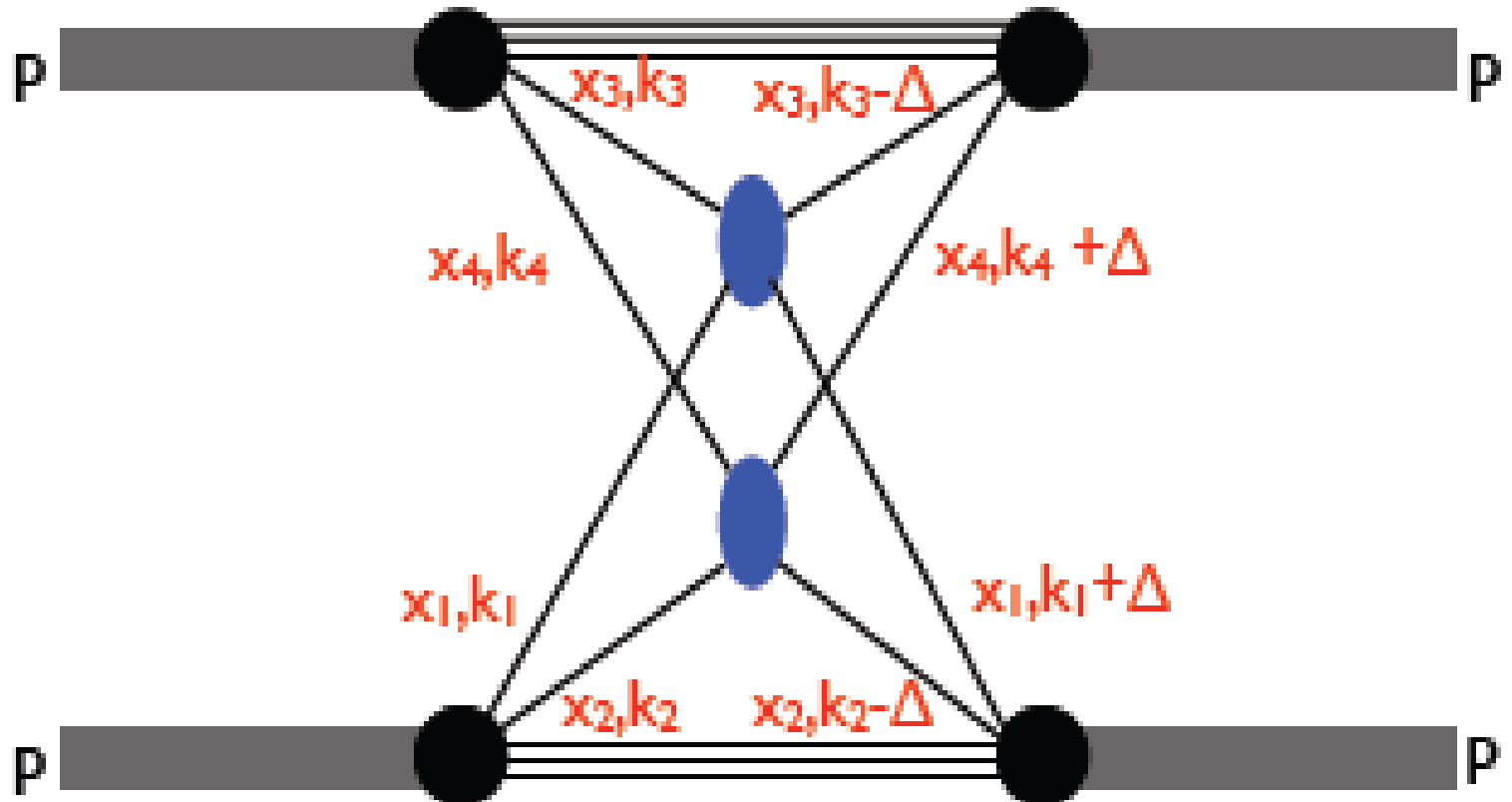
Basic ideas for calculating MPI cross sections in recent years

1. They are expressed via GPD - *BDFS 2010, Diehl 2010*
2. In addition to conventional 4 to 4 mechanism there is also 3 to 4 mechanism
–Fig. 1 b Blok,Dokshitzer,Frankfurt,S trikman (BDFS) 2011,2012,,2013 Ryskin and Snigirev, 2012 Gaunt and Stirling 2011,2012 Manohar and Waalewijn 2012
3. The 4 to 4 contribution is calculated in a model independent way in mean field approximation. *BDFS 2011*
4. Major progress towards factorisation theorem Diehl, Gaunt,Ostermeier,Polessi,Schafer 2015, Diehl,Ostermeier,Schafer 2011

Practically we have to calculate

$$\sigma_{eff} = \frac{\sigma_{eff}^{(0)}}{1 + R},$$

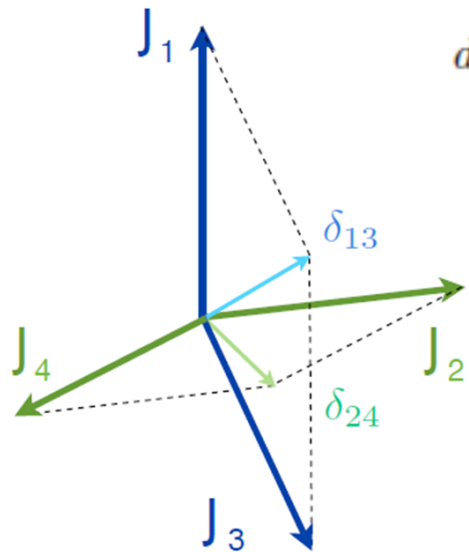
$$\frac{1}{\pi R_{\text{int}}^2} = \int \frac{d^2 \vec{\Delta}}{(2\pi)^2} \frac{D(x_1, x_2, -\vec{\Delta}) D(x_3, x_4, \vec{\Delta})}{D(x_1) D(x_2) D(x_3) D(x_4)}$$



Summing double collinearly enhanced terms

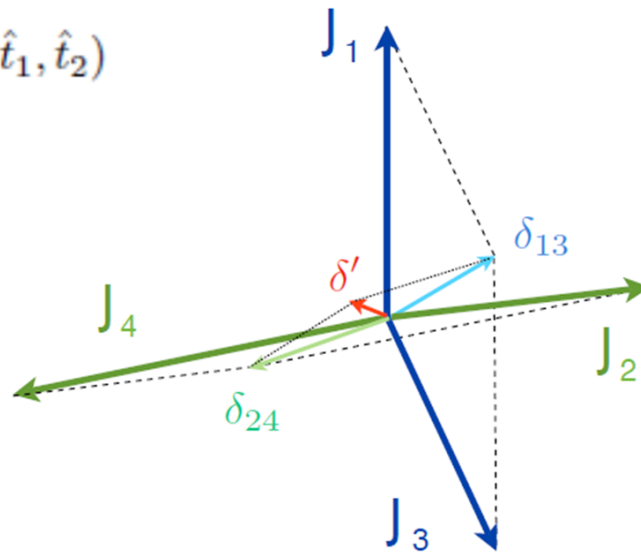
back-to-back kinematics

$$\delta_{13}^2, \delta_{24}^2 \ll J_{i\perp}^2$$



$$d\Sigma(\hat{t}_1, \hat{t}_2)$$

$$\delta'^2 \ll \delta_{13}^2 \simeq \delta_{24}^2 \ll J_{i\perp}^2$$

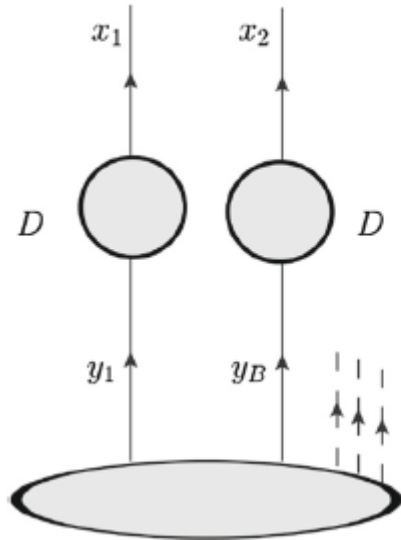


$$d\sigma^{(4 \rightarrow 4)} \propto \frac{\alpha_s^2}{\delta_{13}^2 \delta_{24}^2} d^2 j_{3\perp} d^2 j_{4\perp} \cdot d\Sigma$$

$$d\sigma^{(3 \rightarrow 4)} \propto \frac{\alpha_s^2}{\delta'^2 \delta^2} d^2 j_{3\perp} d^2 j_{4\perp} \cdot d\Sigma$$

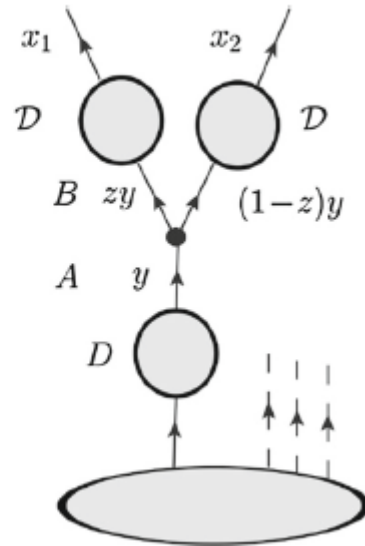
$$[1] D_a^{b,c}(x_1, x_2; q_1^2, q_2^2; \vec{\Delta})$$

$$\begin{aligned} &= \sum_{a', b', c'} \int_{Q_{\min}^2}^{\min(q_1^2, q_2^2)} \frac{dk^2}{k^2} \frac{\alpha_s(k^2)}{2\pi} \\ &\times \int \frac{dy}{y^2} G_a^{a'}(y; k^2, Q_0^2) \\ &\times \int \frac{dz}{z(1-z)} P_{a'}^{b'[c']}(z) G_{b'}^b\left(\frac{x_1}{zy}; q_1^2, k^2\right) \\ &\times G_{c'}^c\left(\frac{x_2}{(1-z)y}; q_2^2, k^2\right). \end{aligned}$$



$$[2] D_a^{b,c}(x_1, x_2; q_1^2, q_2^2; \vec{\Delta})$$

$$\begin{aligned} &= S_b(q_1^2, Q_{\min}^2) S_c(q_2^2, Q_{\min}^2) [2] D_a^{b,c}(x_1, x_2; Q_0^2, Q_0^2; \vec{\Delta}) \\ &+ \sum_{b'} \int_{Q_{\min}^2}^{q_1^2} \frac{dk^2}{k^2} \frac{\alpha_s(k^2)}{2\pi} S_b(q_1^2, k^2) \\ &\times \int \frac{dz}{z} P_{b'}^b(z) [2] D_a^{b',c}\left(\frac{x_1}{z}, x_2; k^2, q_2^2; \vec{\Delta}\right) \\ &+ \sum_{c'} \int_{Q_{\min}^2}^{q_2^2} \frac{dk^2}{k^2} \frac{\alpha_s(k^2)}{2\pi} S_c(q_2^2, k^2) \\ &\times \int \frac{dz}{z} P_{c'}^c(z) [2] D_a^{b,c'}\left(x_1, \frac{x_2}{z}; q_1^2, k^2; \vec{\Delta}\right). \end{aligned} \quad (16)$$



$$D_a^{b,c}(x_1, x_2; q_1^2, q_2^2; \vec{\Delta}) = [2] D_a^{b,c}(x_1, x_2; q_1^2, q_2^2; \vec{\Delta}) + [1] D_a^{b,c}(x_1, x_2; q_1^2, q_2^2; \vec{\Delta})$$

$$\begin{aligned} \frac{1}{\sigma_{eff}} &\equiv \int \frac{d^2 \vec{\Delta}}{(2\pi)^2} [& [2] G_2(x_1, x_3, Q_1^2, Q_2^2; \vec{\Delta}) [2] G_2(x_2, x_4, Q_1^2, Q_2^2; -\vec{\Delta}) \\ & + [1] G_2(x_1, x_3, Q_1^2, Q_2^2; \vec{\Delta}) [2] G(x_2, x_4, Q_1^2, Q_2^2; -\vec{\Delta}) \\ & + [1] G_2(x_2, x_4, Q_1^2, Q_2^2; \vec{\Delta}) [2] G_2(x_1, x_3, Q_1^2, Q_2^2; -\vec{\Delta})]. \end{aligned}$$

2G2 and 1G2 are two parts of GPD ,calculated in two different ways. 2G2-in mean field approach, using GPD1 from charmonium photoproduction at HERA

$$[2] GPD_2(x_1, x_3, Q_1^2, Q_2^2, \Delta) = D_q(x_1, Q_1) D_g(x_3, Q_2) F_{2q}(\Delta, x_1) F_{2g}(\Delta, x_3),$$

$$GPD_{q,g}(x, Q^2, \Delta) = D_{q,g}(x, Q) F_{2g,2q}(\Delta, x).$$

We use parametrisation due to Frankfurt,Strikman,Weiss (2011)

1G2 is calculated solving evolution equation for GPD

The final answer for effective cross section is convenient to represent as

$$\sigma_{eff} = \frac{\sigma_{eff}^{(0)}}{1 + R},$$

Here $\sigma_{eff}^{(0)}$ is the 4 to 4 cross section in mean field approximationwhile the function R corresponds to contribution due to 3 to 4 mechanism, and is calculated analytically.

Note: only one unknown parameter-Q0, separating soft and hard scales, so approach is practically model independent.

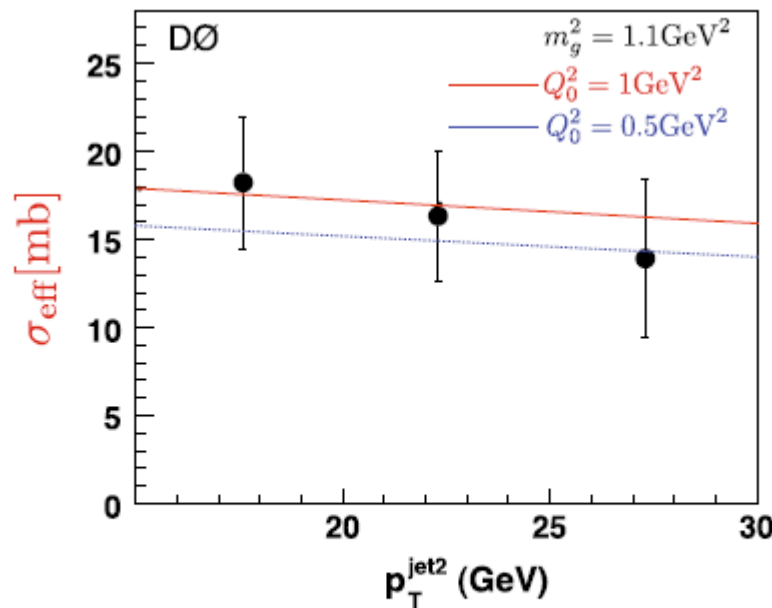
$$F_{2g}(\Delta, x) = \exp(-B_g(x)\Delta^2/2)$$

$B_g(x) = B_0 + 2K_Q \cdot \log(x_0/x)$, with $x_0 \sim 0.0012$, $B_0 = 4.1 \text{ GeV}^{-2}$ and $K_Q = 0.14 \text{ GeV}^{-2}$

$$\frac{1}{\sigma_{eff}^{(0)}} = \frac{1}{2\pi} \frac{1}{B_g(x_1) + B_g(x_2) + B_g(x_3) + B_g(x_4)}.$$

Dipole parametrisation-same results numerically

BDFS 2013, Gaunt, Maciula, Szczerba 2014, Golec-Biernat-Liewandowsky



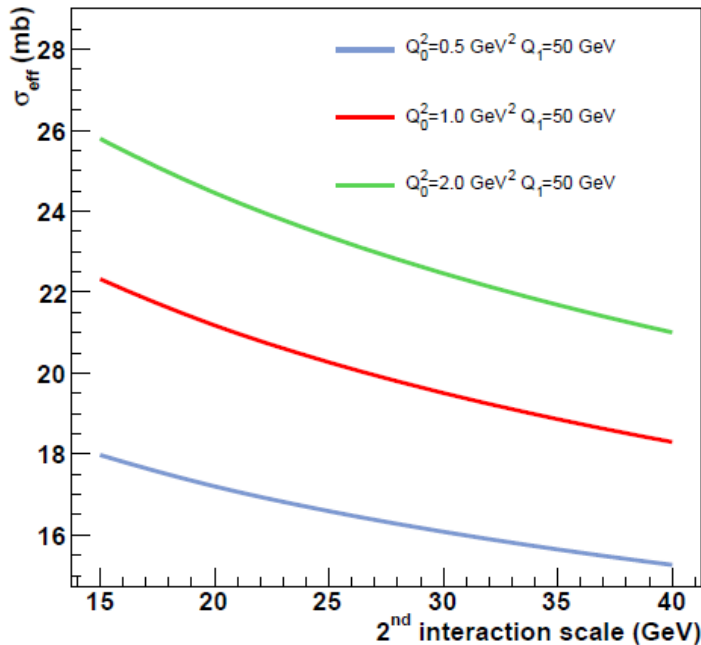


FIG. 10: Values of σ_{eff} as a function of the scale of the 2nd interaction for different scales of the first interaction, Q_1 , and different choices of Q_0^2 . The values of the longitudinal momentum fractions correspond to the maximal transverse momentum exchange.

Table for the values of enhancement R for $Q^2 - Q_1^2 - Q_2^2$, calculated by computer program (see below). The scales Q_1, Q_2 are transverse jet scales. By 3.5x3.5 and 7x7 we mean two different

LHC runs with different s .

Q	$Q_0^2 = 0.5 GeV^2$	$Q_0^2 = 0.5$	$Q_0^2 = 1 GeV^2$	$Q_0^2 = 1$	$Q_0^2 = 2$	$Q_0^2 = 2$
	3.5x3.5	7x7	3.5x3.5	7x7	3.5x3.5	7x7
2.5	0.37	0.34	0.13	0.11	0.04	0.035
5	0.59	0.49	0.26	0.21	0.12	0.11
7.5	0.65	0.59	0.33	0.28	0.18	0.15
10	0.73	0.65	0.4	0.34	0.23	0.19
12.5	0.8	0.71	0.45	0.38	0.27	0.22
15	0.84	0.75	0.5	0.42	0.32	0.25
17.5	0.89	0.79	0.54	0.45	0.34	0.28
20	0.93	0.82	0.58	0.48	0.38	0.3
22.5	0.97	0.86	0.61	0.51	0.41	0.32
25	1.04	0.88	0.64	0.53	0.43	0.35
30	1.07	0.94	0.7	0.58	0.48	0.38
40	1.18	1.02	0.81	0.68	0.58	0.45
50	1.27	1.1	0.9	0.73	0.66	0.51
60	1.36	1.22	1.06	0.85	0.8	0.62
80	1.51	1.27	1.13	0.9	0.87	0.67

these numbers are reasonably approximated by:

first column for $Q^2 > 100$ by $0.089 * \log 2 * Q^2 + 0.0074 * (\log(2 * Q^2))^2$,

second column $0.094 * \log 2 * Q^2 + 0.0045 * (\log(2 * Q^2))^2$,

third column $0.0265 * \log Q^2 + 0.0117 * (\log(Q^2))^2$, and it works virtually everywhere

fourth column $0.0307 * \log Q^2 + 0.00822 * (\log(Q^2))^2$ and it works well,

fifth column $0.0028 * \log Q^2 / 2. + 0.013 * (\log(Q^2 / 2))^2$ works well virtually everywhere

sixth column $0.00866 * \log Q^2 / 2. + 0.009 * (\log(Q^2 / 2))^2$ works well. note that in all this approximations argument of log is $\log(Q^2 / Q_0^2)$

if $Q_1^2 \leq Q_2^2$, then we have $R(Q_1^2, Q_2^2) = R(Q_1^2) + a \text{Log}(Q_2^2, Q_1^2)$, where $R(Q^2)$ is taken from table above, and a is a small number, say for second column $a = 0.035$, I did not check, but I think you can take 0.04, for 1st column, 0.03 for third, 0.025 for fourth, and so on for 5th and 6th columns, the computer evaluated the tables but I did not look into approximations. I think for $Q_0^2 = 0.5$ it is better to use approximation, since we are close to singularity, and the numbers for small Q^2 may

Basic Pythia approach: fit the MPI cross section (and other observables) by using only 4 to 4 contribution in mean field approach and fitting the parameters of the corresponding objects-essentially GPD1. For these GPD1-several ansats,

Simplest-gaussian, more complicated-sum of two gaussians (may be x -dependent). The parameters however are fixed and do not depend on transverse scale. Their optimal values-by combining Pythia and Professor. Problem (P. Gunnellini, Ph.D. thesis): can not have reasonable choice of parameters, valid both for DPS and Underlying event.

The way to solve this problem: include 3 to 4 mechanism, i.e. R not equal to zero, while 4 to 4 contribution will be determined in a model independent way from HERA parametrisation, and not from fit of pp experimental data as in Pythia

Algorithm: take pythia tune, then rescale it on event to event basis, so that effective cross section is given by a theoretical number calculated above.

Several comments:

1. for UE the rescaling coefficients are very small and there is no change (less than 4 percent) for all observables
2. We do not renormalise SPS events.
3. If there are 3 and more dijets in an event, we renormalise as if there are 2 dijets, and take hardest scales.
4. We assume that there is no difference if we use differential cross sections and global ones.

More precisely, one will need
$$\frac{\pi^2 d\sigma^{\text{DPI}}}{d^2 \delta_{13} d^2 \delta_{24}}^c$$

Pythia 4 jet simulation.

We first did conventional

pythia 8 simulation

PYTHIA 8 Parameter	Value obtained for the UE tune
MultipleInteractions: p_T^0 Ref	2.659
BeamRemnants:reconnectRange	3.540
Reduced χ^2	0.647
σ_{eff} (7 TeV) (mb)	29.719
σ_{eff} (14 TeV) (mb)	32.235

UE observables:

Transverse N_{chg} density vs. p_{\perp}^{trk1} , $\sqrt{s} = 7$ TeV

Transverse $\sum p_{\perp}$ density vs. p_{\perp}^{trk1} , $\sqrt{s} = 7$ TeV

$$\Delta S = \arccos \left(\frac{\vec{p}_T(\text{pair}_1) \cdot \vec{p}_T(\text{pair}_2)}{|\vec{p}_T(\text{pair}_1)| \times |\vec{p}_T(\text{pair}_2)|} \right),$$

DPS observables

$$\Delta^{rel} p_T = \frac{|\vec{p}_T^{jet_1} + \vec{p}_T^{jet_2}|}{|\vec{p}_T^{jet_1}| + |\vec{p}_T^{jet_2}|},$$

Several simulations for 4 jets:

- “UE tune”: predictions obtained with the parameters listed in Table I and without applying any reweighting of the simulation; this tune uses a constant value of σ_{eff} , following the standard PYTHIA approach;
- “UE tune Q^2 -dep”: predictions obtained with the UE parameters listed in Table I and by applying the scale dependence of σ_{eff} with $Q_0^2 = 1 \text{ GeV}^2$;
- “UE tune x -dep”: predictions obtained with the UE parameters listed in Table I and by applying the x dependence of σ_{eff} ;
- “UE tune Dynamic σ_{eff} ”: predictions obtained with the UE parameters listed in Table I and by applying both the x and the scale dependence with $Q_0^2 = 1 \text{ GeV}^2$.

For the considered “UE tune Dynamic σ_{eff} ”, predictions using Q_0^2 values equal to 0.5, 1 and 2 GeV^2 have been also tested and compared.

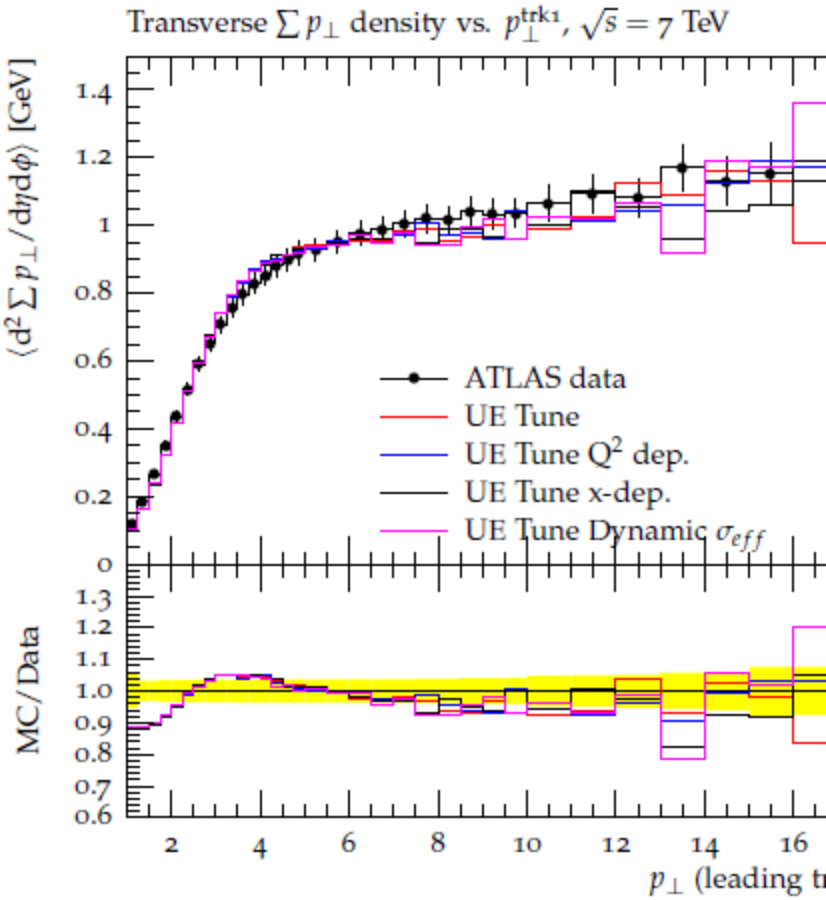
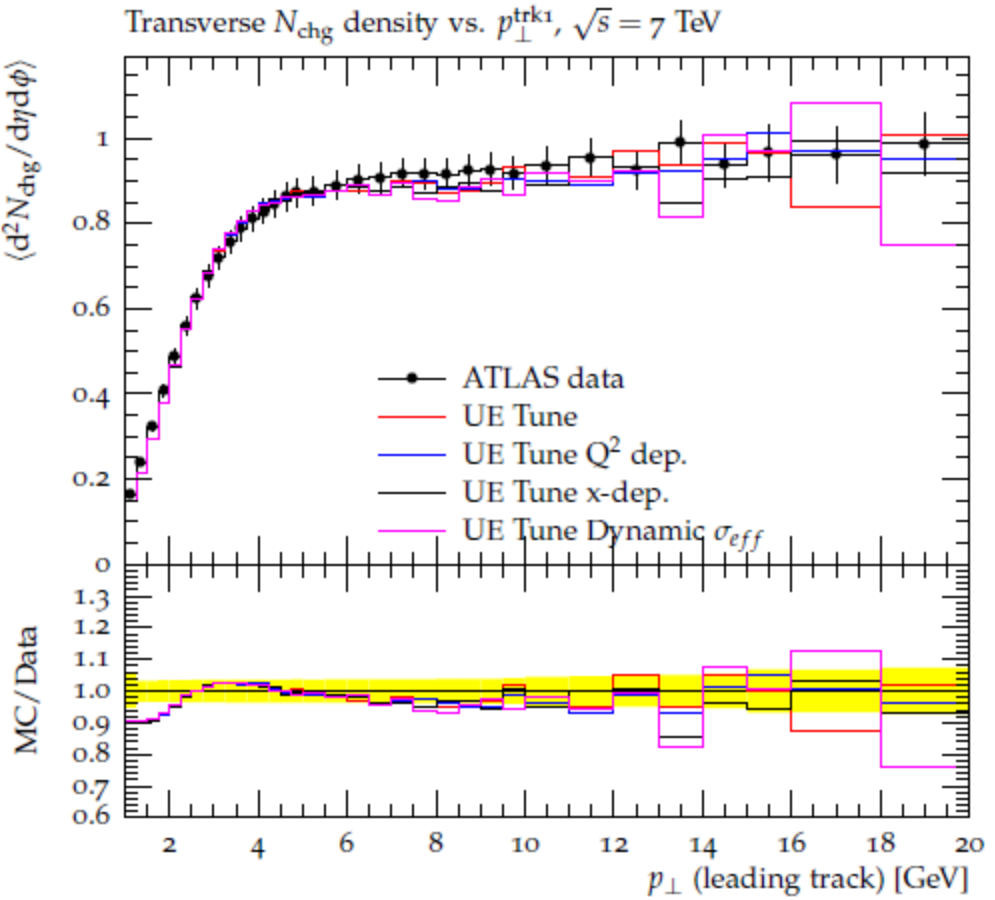


FIG. 2: Charged particle density (left) and p_T sum density (right) as a function of the leading charged particle's transverse momentum in the transverse regions, measured by the ATLAS experiment at 7 TeV [39]. The data are compared with various predictions: the UE tune with constant σ_{eff} value (red curve), the UE tune with σ_{eff} x -dependence (blue curve), the UE tune with σ_{eff} scale dependence with $Q_0^2=1.0$ GeV 2 applied (black curve), and the UE tune with both σ_{eff} x and scale dependence with $Q_0^2=1.0$ GeV 2 applied (pink curve). The ratio panel shows the ratio between the various prediction and the experimental points.

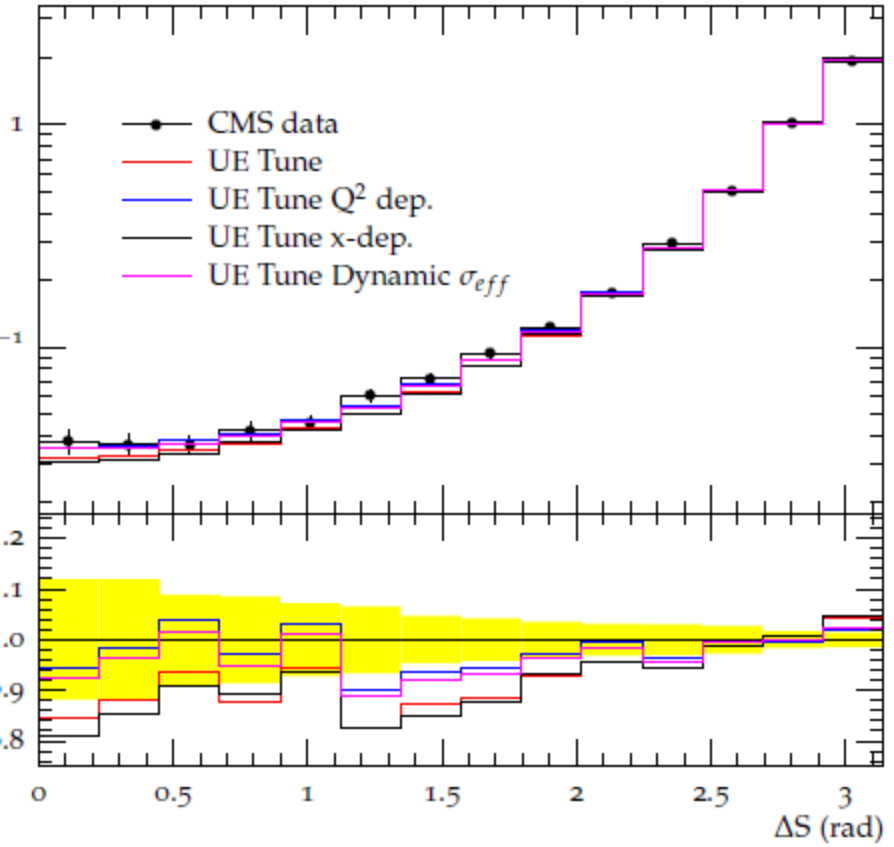
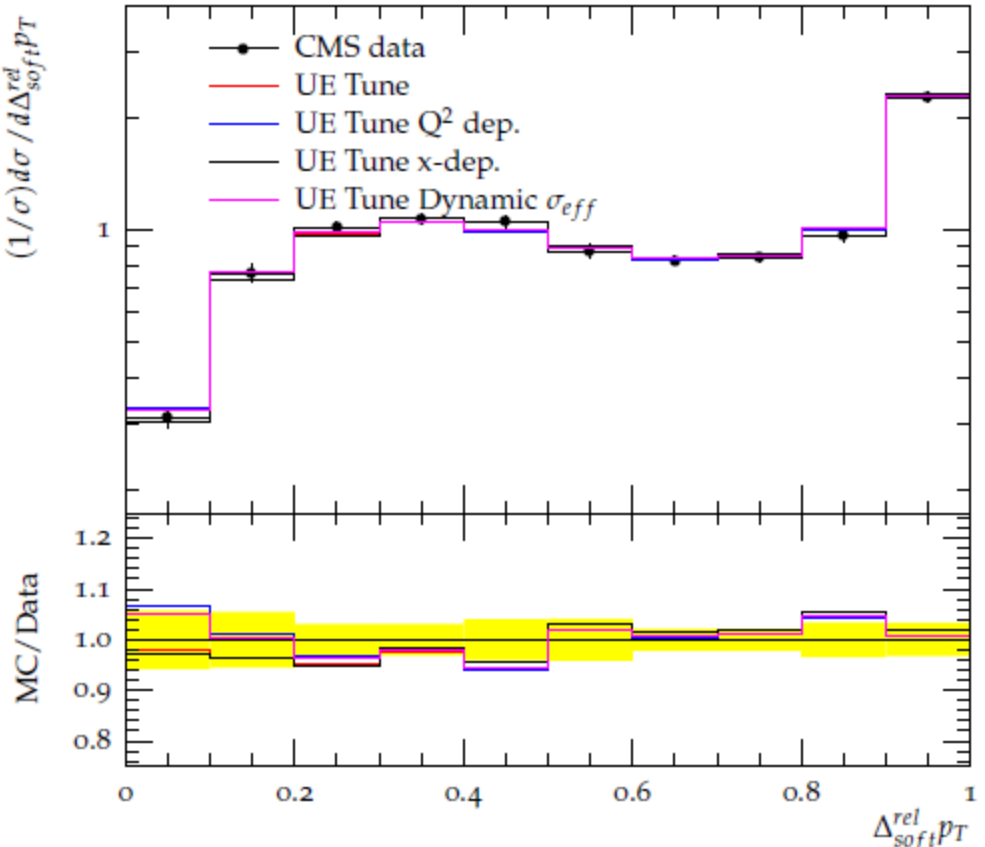
Normalized ΔS in $pp \rightarrow 4j$ in $|\eta| < 4.7$ at $\sqrt{s} = 7$ TeVNormalized $\Delta_{soft}^{rel} p_T$ in $pp \rightarrow 4j$ in $|\eta| < 4.7$ at $\sqrt{s} = 7$ TeV

FIG. 4: Normalized cross section distributions as a function of the correlation observables ΔS (left) and $\Delta_{soft}^{rel} p_T$ (right) measured in a four-jet scenario by the CMS experiment at 7 TeV [38]. The data are compared to various predictions: the new UE tune (red curve), the new UE tune with the x dependence applied (blue curve), the new UE tune with only the scale dependence with $Q_0^2=1.0$ GeV 2 applied (black curve) and the new UE tune with both x and scale dependence with $Q_0^2=1.0$ GeV 2 applied (pink curve). The lower panel shows the ratio between the various prediction and the experimental points.

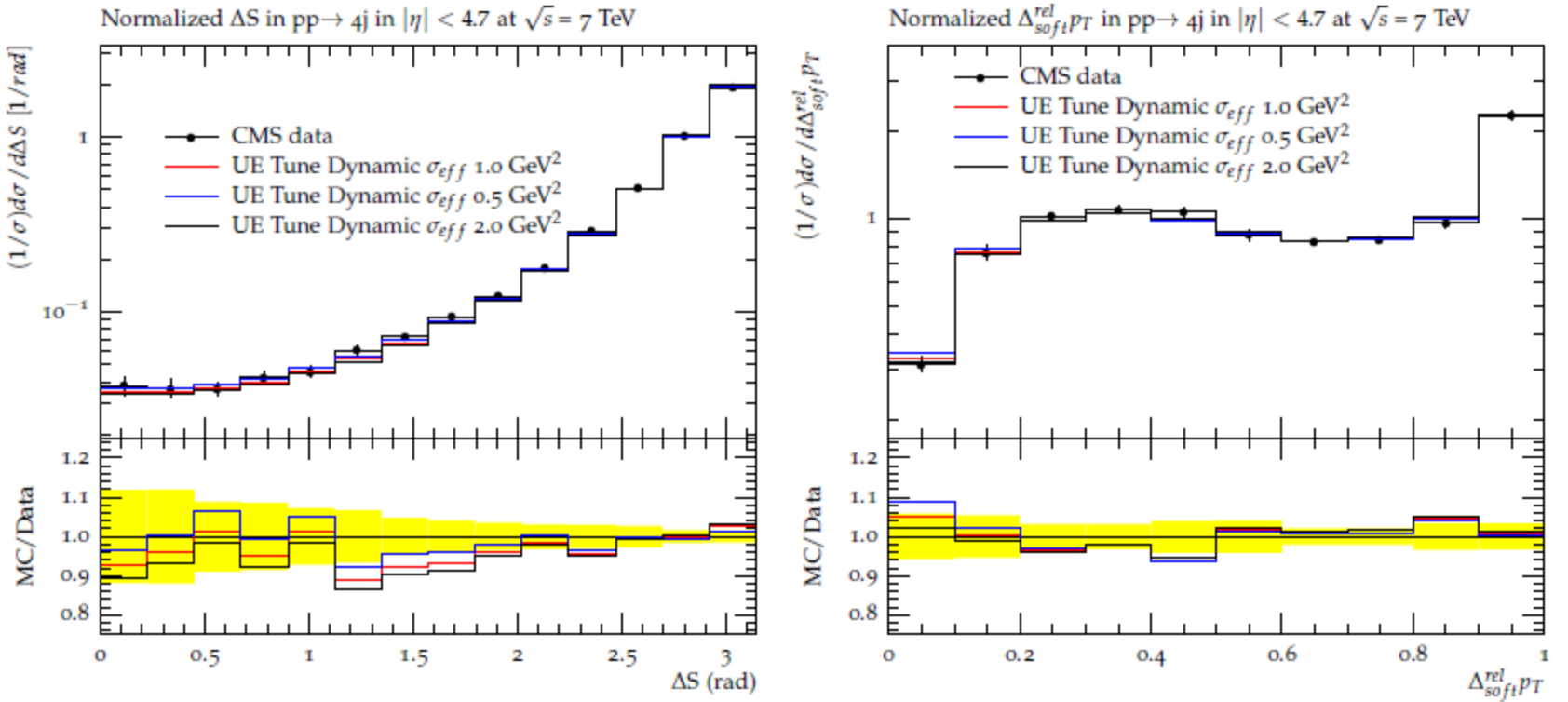


FIG. 5: Normalized cross section distributions as a function of the correlation observables ΔS (left) and $\Delta_{soft}^{rel} p_T$ (right) measured in a four-jet scenario by the CMS experiment at 7 TeV [38]. The data are compared to various predictions obtained with the new UE tune where both x and scale dependence have been applied with Q_0^2 equal to 1.0 (red curve), 0.5 (blue curve) and 2.0 (black curve) GeV^2 . The lower panel shows the ratio between the various prediction and the experimental points.

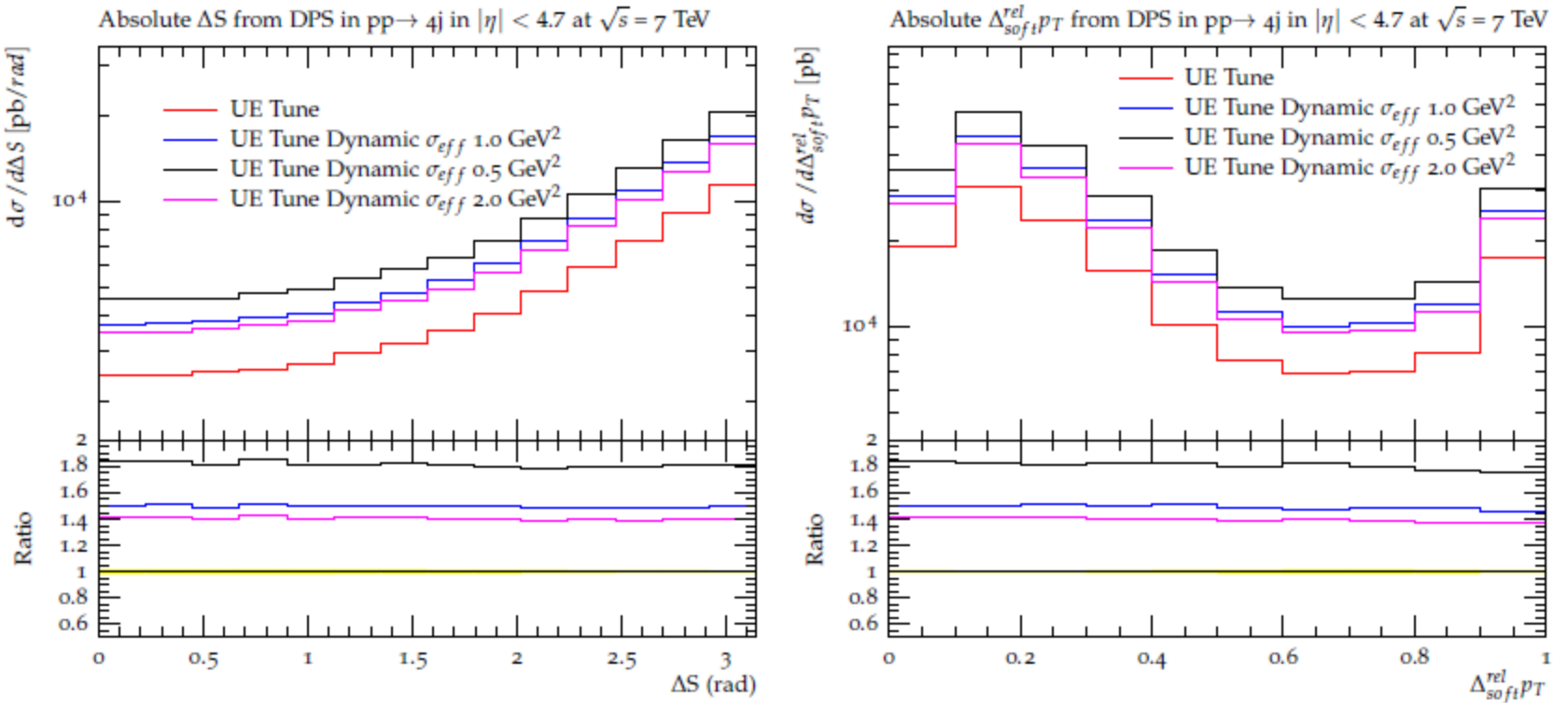


FIG. 6: Absolute cross section distributions as a function of the correlation observables ΔS (left) and $\Delta_{soft}^{rel} p_T$ (right), produced via double parton scattering in a four-jet scenario at 7 TeV. Various predictions are shown in the figures: the new UE tune (red curve), the new UE tune with the x dependence applied (blue curve), the new UE tune with only the scale dependence with $Q_0^2=1.0$ GeV 2 applied (black curve) and the new UE tune with both x and scale dependence with $Q_0^2=1.0$ GeV 2 applied (pink curve). The lower panel shows the ratio between the various predictions and the predictions obtained with the new UE tune.

Now consider Zjj and Wjj MPI

DPS observables:

$$\Delta S = \arccos \left(\frac{\vec{p}_T(\text{boson}) \cdot \vec{p}_T(\text{jet}_{1,2})}{|\vec{p}_T(\text{boson})| \times |\vec{p}_T(\text{jet}_{1,2})|} \right),$$

$$\Delta^{\text{rel}} p_T = \frac{|\vec{p}_T^{\text{jet}_1} + \vec{p}_T^{\text{jet}_2}|}{|\vec{p}_T^{\text{jet}_1}| + |\vec{p}_T^{\text{jet}_2}|},$$

UE observables

- charged particle multiplicity density (N_{ch});
- transverse momentum sum density (Σp_T).

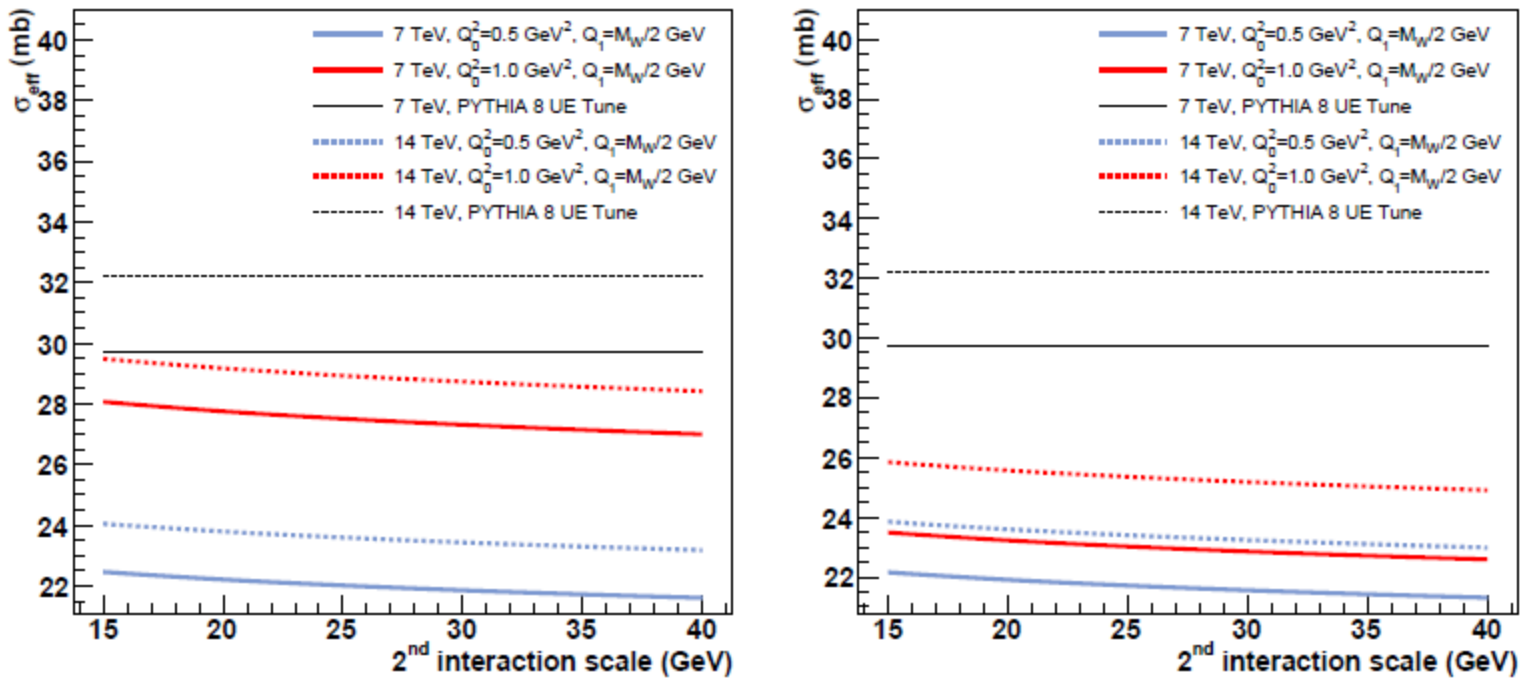


FIG. 10: Values of σ_{eff} as a function of the scale of the 2nd interaction at different collision energies at 7 TeV and 14 TeV for first hard interactions occurring at a scale Q_1 equal to $M_W/2$ and $M_Z/2$ GeV for, respectively, Wjj (*left*) and Zjj (*right*) channels. The two values of Q_0^2 equal to 0.5 and 1.0 GeV^2 are considered and the longitudinal momentum fractions of the two dijets correspond to the maximal transverse momentum exchange for both $\sqrt{s} = 7$ TeV and $\sqrt{s} = 14$ TeV. Also shown are the values of σ_{eff} for each energy, as implemented in the PYTHIA 8 UE Tune if no reweighting is applied.

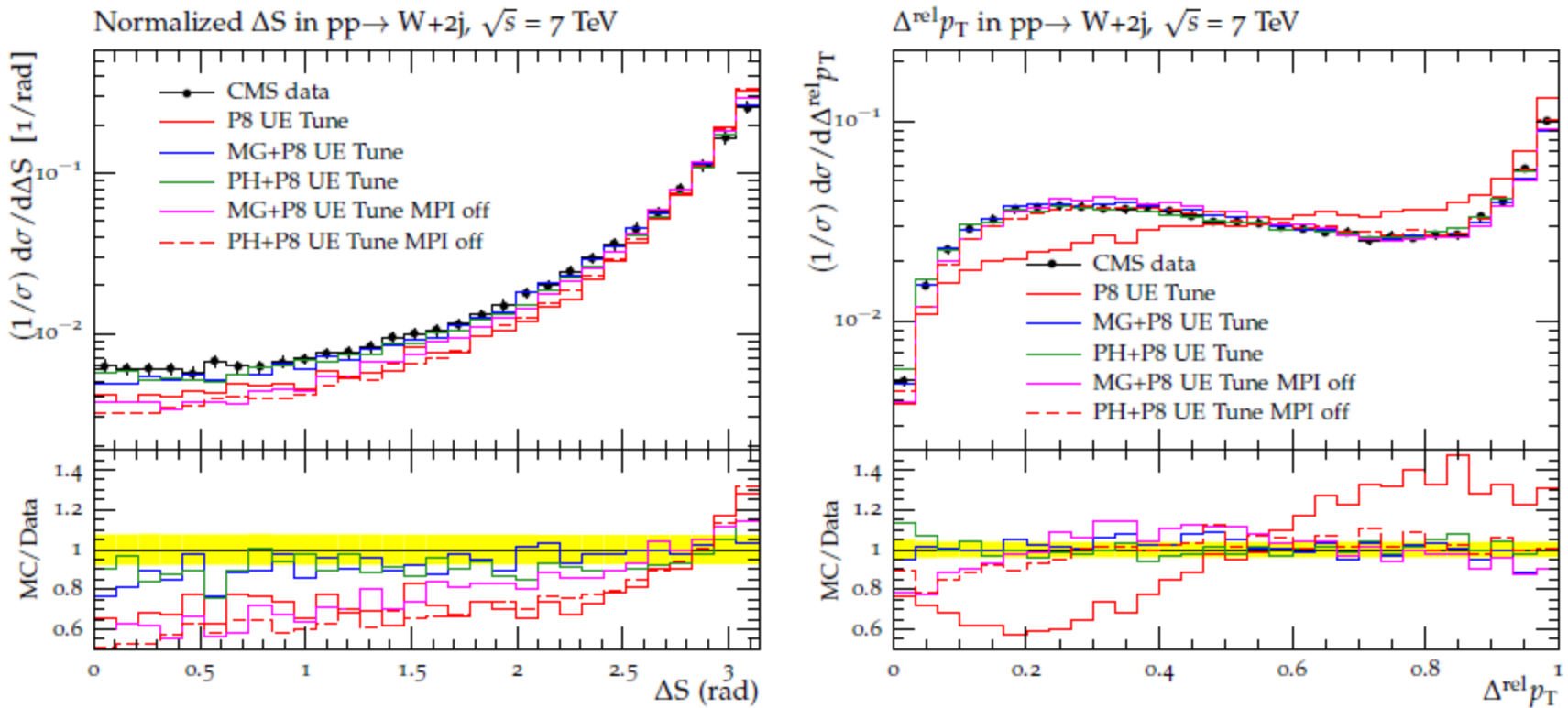


FIG. 2: CMS data [37] at 7 TeV for the normalized distributions of the correlation observables ΔS (*left*) and $\Delta^{\text{rel}} p_T$ (*right*) in the $W+\text{dijet}$ channel, compared to predictions generated with PYTHIA 8 UE Tune, MADGRAPH and POWHEG interfaced to PYTHIA 8 UE Tune. Predictions obtained with MADGRAPH and POWHEG interfaced to PYTHIA 8 UE Tune, without the simulation of the MPI are also compared to the measurement. The ratios of these predictions to the data are shown in the lower panels.

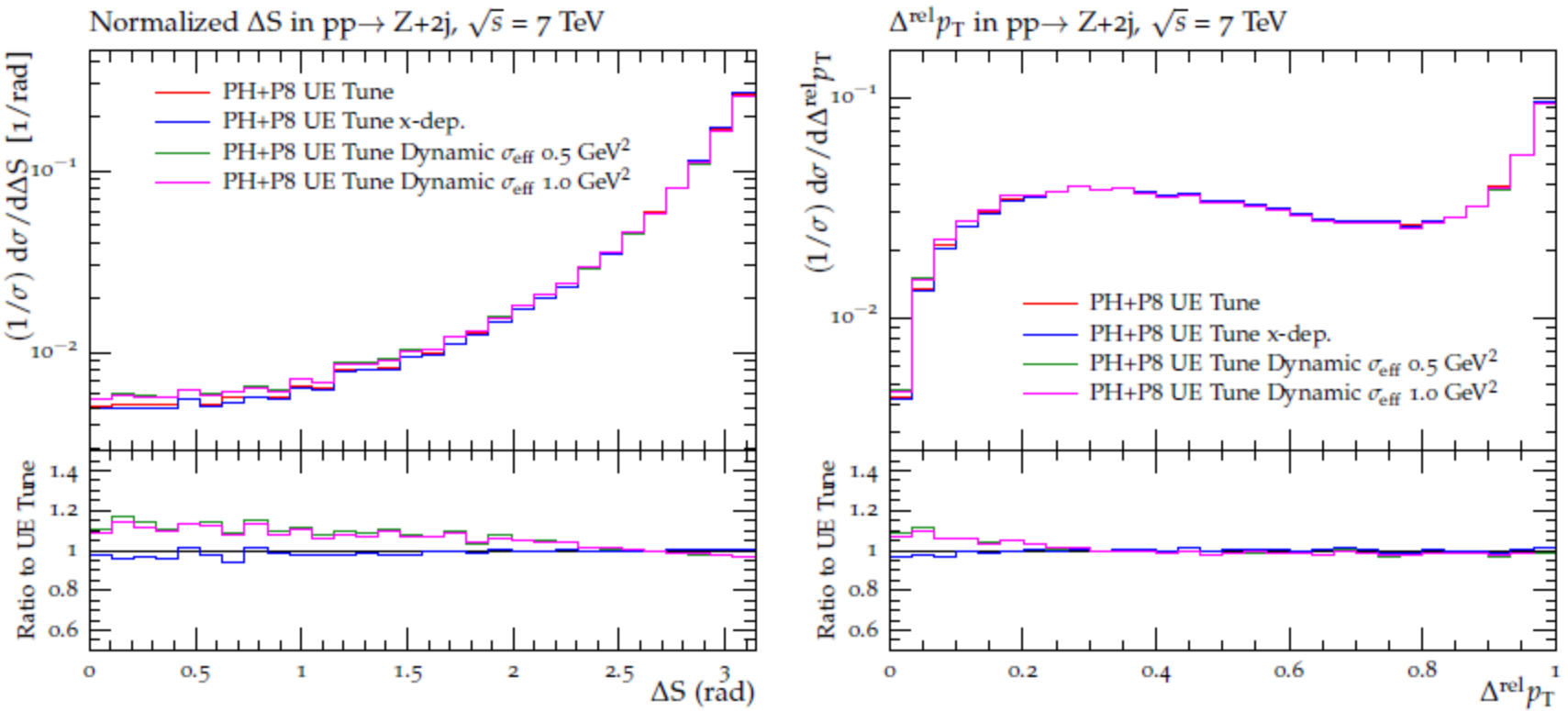


FIG. 4: Predictions at 7 TeV for the normalized distributions of the correlation observables ΔS (*left*) and $\Delta^{\text{rel}} p_T$ (*right*) in the Z+dijet channel, of simulations performed with POWHEG interfaced to PYTHIA 8 UE Tune with different σ_{eff} dependence applied: no σ_{eff} reweighting applied (red line), x -dependent σ_{eff} values (blue line), x - and scale-dependent σ_{eff} values with $Q_0^2 = 0.5 \text{ GeV}^2$ (green line) and x - and scale-dependent σ_{eff} values with $Q_0^2 = 1 \text{ GeV}^2$ (pink line). Also shown are the ratios of each curve to the predictions of the UE Tune.

Predictions obtained with the considered tunes are also tested for UE observables in inclusive W and Z boson events. This kind of events are sensitive to MPI at moderate scales. In Fig. 5, predictions on charged-particle multiplicity and p_T sum densities are shown for inclusive W events in the transverse region as a function of the W-boson p_T . Curves obtained with POWHEG interfaced to PYTHIA 8 UE Tune and implementing different σ_{eff} dependence differ less than 2% from each other. This effect is very similar to the one observed in hadronic events, documented in [43].

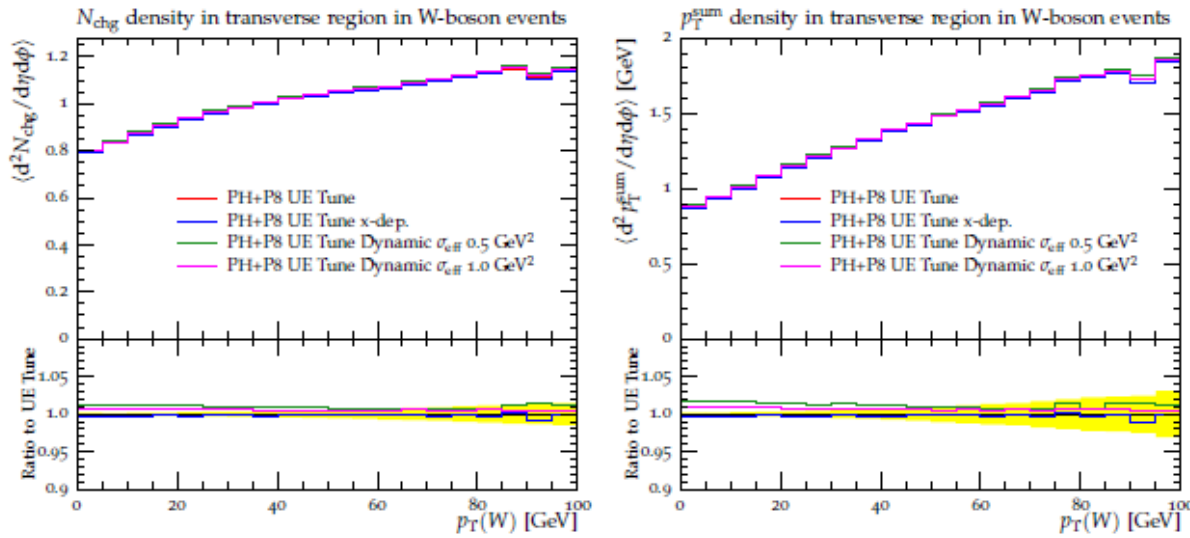


FIG. 5: Predictions for the (*left*) charged-particle and (*right*) p_T sum densities in the transverse regions as defined by the W-boson in proton-proton collisions at 7 TeV. Simulations obtained with POWHEG interfaced to PYTHIA 8 UE Tune are considered with different σ_{eff} dependence applied: no reweighting applied (red line), x -dependent σ_{eff} values (blue line), x - and scale-dependent σ_{eff} values with $Q_0^2 = 0.5 \text{ GeV}^2$ (green line) and x - and scale-dependent σ_{eff} values with $Q_0^2 = 1 \text{ GeV}^2$ (pink line). Also shown are the ratios of these tunes to the predictions of the UE Tune.

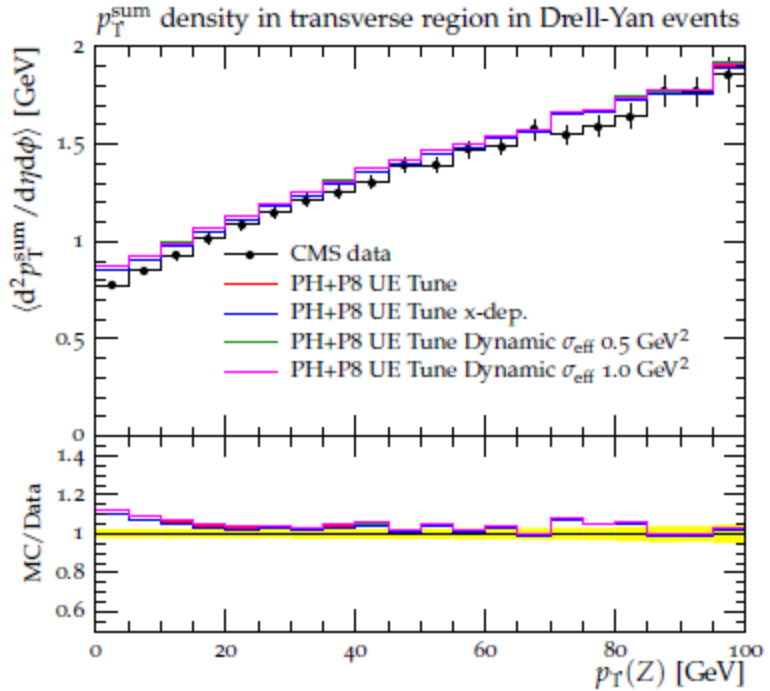
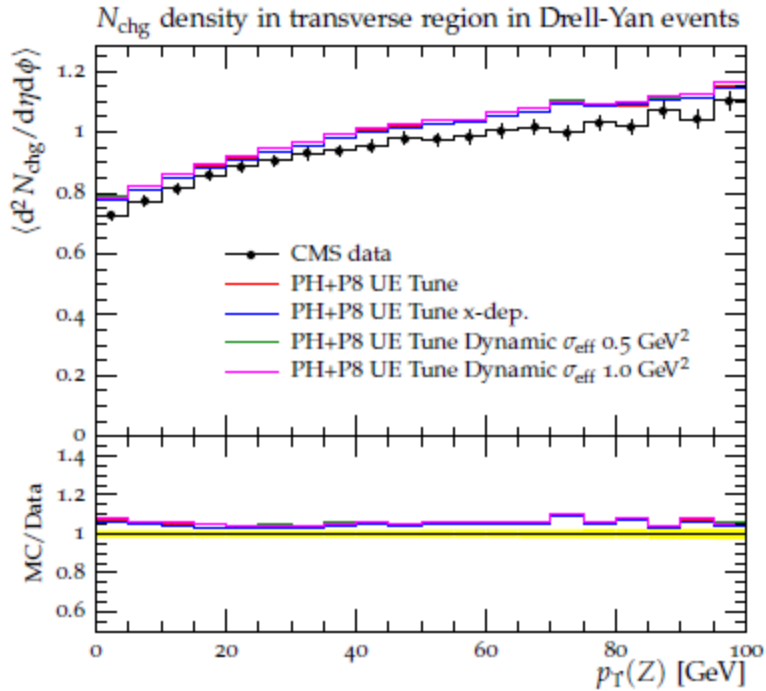
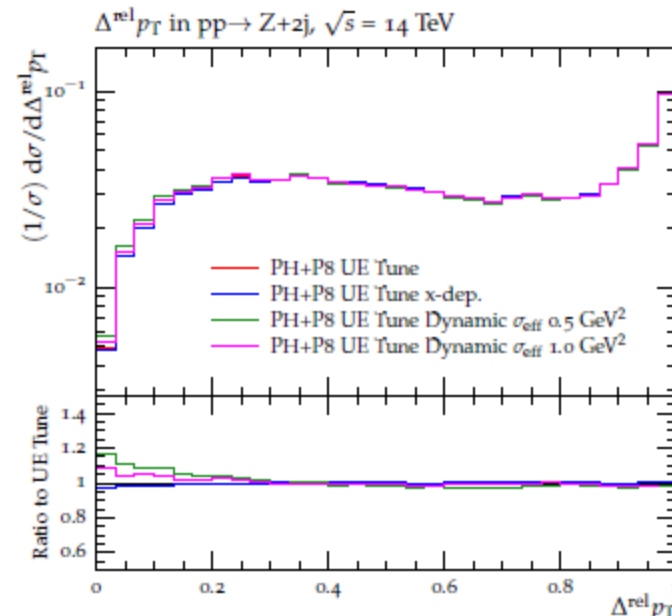
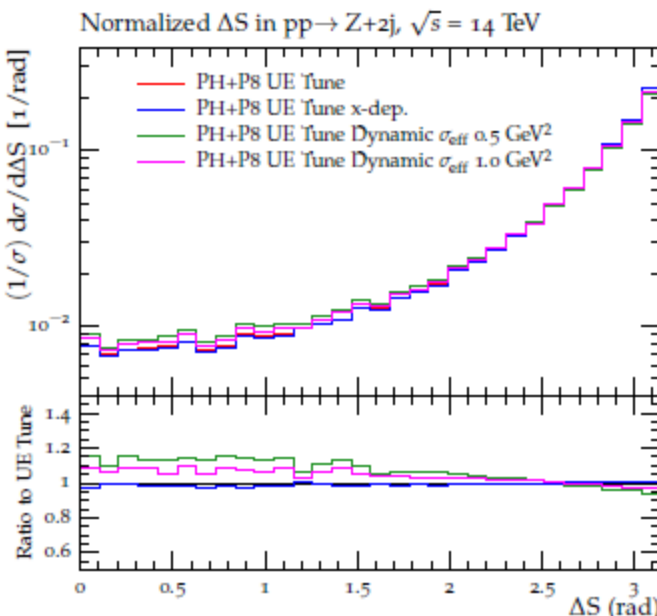
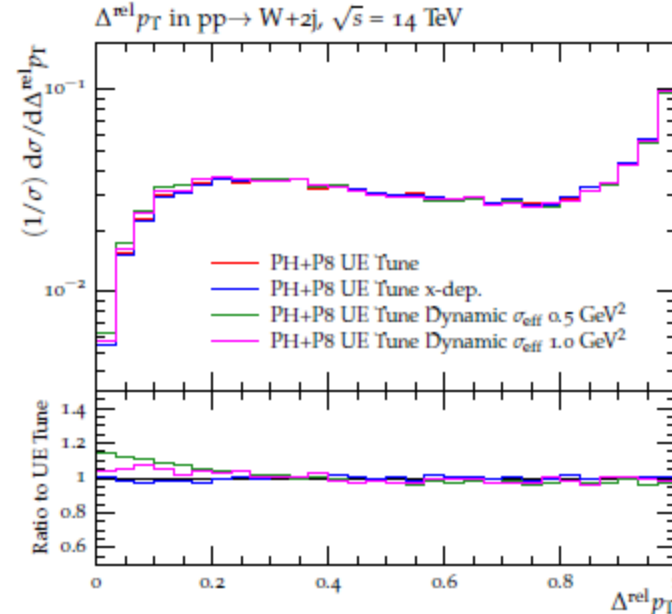
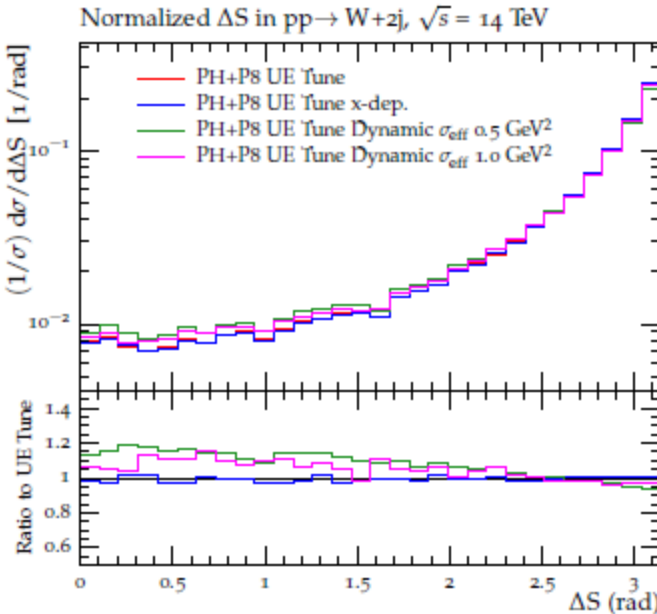


FIG. 6: CMS data [50] for the (*left*) charged-particle and (*right*) p_T sum densities in the transverse region as defined by the Z-boson in Drell–Yan production in proton-proton collisions at 7 TeV. The data are compared to POWHEG interfaced to PYTHIA 8 UE Tune with different σ_{eff} dependence applied: no reweighting applied (red line), x -dependent σ_{eff} values (blue line), x - and scale-dependent σ_{eff} values with $Q_0^2 = 0.5 \text{ GeV}^2$ (green line) and x - and scale-dependent σ_{eff} values with $Q_0^2 = 1 \text{ GeV}^2$ (pink line). Also shown are the ratios of these tunes to the data.

14 TeV predictions for Wjj and Zjj DPS



Conclusions

- We can calculate DPS in a model independent way (upto Q0 dependence)
- The inclusion of 3 to 4 mechanism improves the agreement between experiment and MC simulations in all observables. The contribution is negligible for UE but large for DPS
- Further improvement is possible, in particular moving from global rescaling to differential one, using differential distributions $\frac{d\sigma}{d^2\delta_{13} d^2\delta_{24}}$, written in BDFS 2011,2013

The approach can be extended to other processes including charm and bottom states

<http://desy.de/~gunnep/SigmaEffectiveDependence/>.